

Numerical solution of three dimensional unsteady biomagnetic flow and heat transfer through stretching/shrinking sheet using temperature dependent magnetization

M. G. MURTAZA¹⁾, E. E. TZIRTZILAKIS²⁾, M. FERDOWS¹⁾

¹⁾*Research Group of Fluid Flow Modeling and Simulation
Department of Applied Mathematics
University of Dhaka
Dhaka-1000, Bangladesh
e-mails: ferdows@du.ac.bd*

²⁾*Fluid Dynamics & Turbomachinery Laboratory
Department of Mechanical Engineering
Technological Educational Institute of Western Greece
1 M. Aleksandrou St.
Koukoulis, 26334 Patras, Greece*

THE PROBLEM OF BIOMAGNETIC FLUID FLOW AND HEAT TRANSFER in the three-dimensional unsteady stretching/shrinking sheet is examined. Our model is the version of biomagnetic fluid dynamics (BFD) which is consistent with the principles of ferrohydrodynamics (FHD). Our main contribution is the study of the three dimensional time dependent BFD flow which has not been considered yet to our best knowledge. The physical problem is described by a coupled, nonlinear system of ordinary differential equations subject to appropriate boundary conditions. The solution is obtained numerically by applying an efficient numerical technique based on the finite difference method. Computations are performed for a wide range of the governing parameters such as ferromagnetic interaction parameter, unsteadiness parameter, stretching parameter and other involved parameters. The effect of these parameters on the velocity and temperature fields are examined. We observed that for the decelerated flow, the velocity profile overlap with the increasing unsteadiness parameter and we also found that the skin friction coefficient is decreased for a shrinking sheet whereas, opposite behavior is shown for the stretching sheet. We also monitored the rate of the heat transfer coefficient with the ferromagnetic interaction parameter and showed opposite behavior for stretching and shrinking sheets. Our results are also compared for specific values of the parameters with others documented in literature.

Key words: biomagnetic fluid, ferro fluid, stretching/shrinking sheet, magnetic dipole.

Notation

(x, y, z)	Cartesian coordinates, m,
(u, v, w)	velocity components in the x, y, z direction, m,
(ξ, ζ, η)	non-dimensional coordinates,
p	fluid pressure, $\text{kg/m} \cdot \text{s}^2$,
\vec{M}	magnetization, A/m,
H	magnetic field intensity, A/m,
B	magnetic induction, A/m,
B_s	saturation magnetic induction, A/m,
M_s	saturation magnetization, A/m,
T	fluid temperature inside the boundary layer, K,
T_c	fluid temperature far away from sheet, K,
T_w	temperature of the sheet, K,
P_1, P_3, P_5	dimensionless pressure,
(f', g')	dimensionless velocity components in the x and y directions,
$(\theta_1, \theta_3, \theta_5)$	dimensionless temperature,
ρ	density of fluid, kg/m^3 ,
μ	dynamic viscosity, $\text{kg}/(\text{m} \cdot \text{s})$,
ν	kinematic viscosity, m^2/s ,
μ_0	magnetic permeability, $\text{kg} \cdot \text{m}/(\text{A}^2 \cdot \text{s}^2)$,
A	unsteadiness parameter
C_p	Specific heat constant pressure, $\text{J}/(\text{kg} \cdot \text{K})$,
k	thermal conductivity, $\text{J}/(\text{m} \cdot \text{s} \cdot \text{K})$,
a	dimensionless constant,
λ	stretching parameter,
Pr	Prandtl number
λ_a	viscous dissipation parameter,
ε	dimensionless Curie temperature,
β	ferromagnetic interaction parameter,
δ	dimensionless distance,
φ	dissipation function.

1. Introduction

WHEN THE HUMAN BODY IS MOVING to the various environments, such as travelling or any hard working then the body is accelerated or decelerated with time and space. The flow behavior of blood and the temperature are also changed in time. Generally speaking, capillaries carry the blood through skin and muscles and arteries carry the blood away from the heart whereas veins carry the blood towards the heart. Also it is known that, muscles, arteries and veins are stretched continuously and as a first approximation we could consider muscles as a stretching/shrinking surfaces and arteries or veins as a stretching/shrinking cylinders. So, one could consider, blood flow applicable to stretching/shrinking surfaces. In such situations the blood flow of artery is unsteady and heat transfer is occurring from a surface of tissues, skin or body by sweating or conducting. The most common example of biomagnetic fluid existing in a living

creature is blood. Since the body always moves in various positions all the time, the unsteady state condition analysis is of significant importance for the flow problem.

The influence of the magnetic field on biofluid flow has been extensively investigated for bioengineering and medical applications [1–3], particularly for controlling blood flow for surgery, cancer treatment, drug targeting etc. The mathematical model for a ferrofluid flow (FHD) over a stretching sheet was used by ANDERSSON and VALNES [4] and found that the flow has significantly affected in the presence of a magnetic dipole. YESMEEN *et al.* [5] investigated the flow and heat transfer of ferrofluid over a stretched surface and reported that the velocity profile decreases due to the increment of the magnetic number. ZEESHAN *et al.* [6] studied ferrofluid flow over a stretching sheet and investigated the effect of a magnetic dipole on the flow behavior. MAJEED *et al.* [7] studied the unsteady ferromagnetic flow over a stretching sheet with prescribed heat flux. ZEESHAN *et al.* [8] analyzed the boundary layer heat transport flow of multiphase magnetic fluid with solid impurities suspended homogeneously past a stretching sheet under the impact of circular magnetic field. MAJEED *et al.* [9] studied the influence of chemical reaction and heat transfer analysis of Maxwell saturated Ferrofluid flow over a stretching sheet under the influence of a magnetic dipole with Soret and suction effects. BHATTI *et al.* [10] reported the entropy generation on electro kinetically modulated peristaltic propulsion on magnetized nanofluid flow through a microchannel with joule heating.

Many authors have investigated the blood flow and heat transfer under the action of external magnetic field. HAIK *et al.* [11] first introduced the mathematical model of BFD. This model is based on the principles of FHD [12]. Further, an extended BFD mathematical model was developed by TZIRTZILAKIS [13] based on both principles of FHD and MHD.

The magnetic field strength H which is generated by a magnetic dipole, is affecting the fluid flow and the significant magnetization M is attained when the magnetic field is sufficiently strong to saturate the biomagnetic fluid. There are various magnetization equations describing M . ANDERSSON and VALNES [4] considered a magnetization equation varying linearly with temperature whereas, TZIRTZILAKIS and KAFOUSSIAS [14] considered a nonlinear magnetization equation. HAIK *et al.* [33] studied the variation of blood viscosity in a human body under the action of a high static magnetic field. For their model they used a magnetization equation which was not temperature dependent.

Furthermore, mathematical models have been developed for blood flow and many authors like ELDESOKY [15] assumed blood as a Newtonian fluid. Moreover, ELDESOKY [15] studied the MHD blood flow of an unsteady parallel plate in the presence of a heat source. MISRA and SINHA [16] studied the MHD flow of blood in a capillary with lumen being porous and wall permeable. TZIRTZILAKIS

and KAFOUSSIAS [17] investigated the magnetic fluid (FHD) flow over a three dimensional stretching sheet.

SINGH and RATHEE [18] studied the blood flow through an artery in the presence of the magnetic field with variable blood viscosity. Under the periodic body movement, the MHD pulsatile flow was presented by DAS and SAHA [19]. DULAL and ANANDA [20] investigated the blood flow through an artery in the presence of the magnetic field. Unsteady MHD blood flow through a parallel plate was studied by ALI *et al.* [21].

Initially, most of the researchers studied steady flows over a stretching sheet. However, the interest of the unsteady flow over a shrinking sheet has considerably increased among researchers. BACHOK *et al.* [22] and FANG *et al.* [23] studied the unsteady fluid flow over a stretching/shrinking sheet and they emphasized the deviation in flow behaviors for an unsteady shrinking sheet compared with those observed for an unsteady stretching sheet. BHATTI and RASHIDI [24] described the combined effect of thermos-diffusion and thermal radiation on Williamson nanofluid over a porous stretching sheet. Further, BHATTI and RASHIDI [25] reported the entropy generation with nonlinear thermal radiation in the MHD boundary layer flow over a permeable shrinking/stretching sheet. BHATTI *et al.* [26] analyzed the flow over a permeable shrinking sheet under the influence of MHD. DANDAPAT *et al.* [27] analyzed the problems of heat transfer due to a permeable stretching wall in the presence of transverse magnetic field. NIKODIJEVIC *et al.* [28] presented a parametric method for the unsteady two-dimensional MHD boundary-layer on a body for which temperature varies with time. MAJEED *et al.* [29] examined the boundary layer flow of a nanofluid due to a magnetic dipole over a stretching surface with the velocity slip condition. MISHRA *et al.* [30] analyzed mass and heat transfer over an electrically conducting viscoelastic fluid over a stretching surface in the presence of the transverse magnetic field. SHEIKOLESLAMI and BHATTI [31] studied the forced convective heat transfer in a porous semi-annulus in the presence of a uniform magnetic field. HASSAN *et al.* [32] analyzed the nanoparticle shapes behavior on ferrofluid flow and heat transfer over a rotating disk with the presence of the oscillating magnetic field.

In the present paper we study the BFD flow and heat transfer of blood along a stretching/shrinking three dimensional sheet. For the mathematical formulation we adopt the version of BFD which is consistent with the FHD principles. The transformed similarity equations are solved numerically using a finite different scheme with central differencing. The influence of the physical controlling parameter on velocity and temperature profiles is elucidated through the graphs. Also, we computed the missing slopes. The hope is that the present analysis will be used in bio-medical and bio-engineering applications. Furthermore, comparison of the numerical findings is performed within some limitations with existing results.

2. Problem formulation and basic equations

We consider an unsteady three dimensional incompressible, viscous, laminar biomagnetic fluid past a stretching/shrinking sheet whose flow direction in the coordinate system is taking place in the (x, y, z) plane with velocities $U(x, t) = U_w(x, t)$, $V(y, t) = V_w(y, t)$ and $w(z, t) = 0$ whereas, z is perpendicular to the (x, y) plane (Fig. 1). Assume that the fluid occupies the upper half plane $z \geq 0$. The flow field is subject to the presence of a magnetic field generated by a magnetic wire which is located below the sheet at a distance d . The temperature of the sheet T_w is kept fixed and T_c is the temperature far away from the sheet, with $T_w < T_c$.

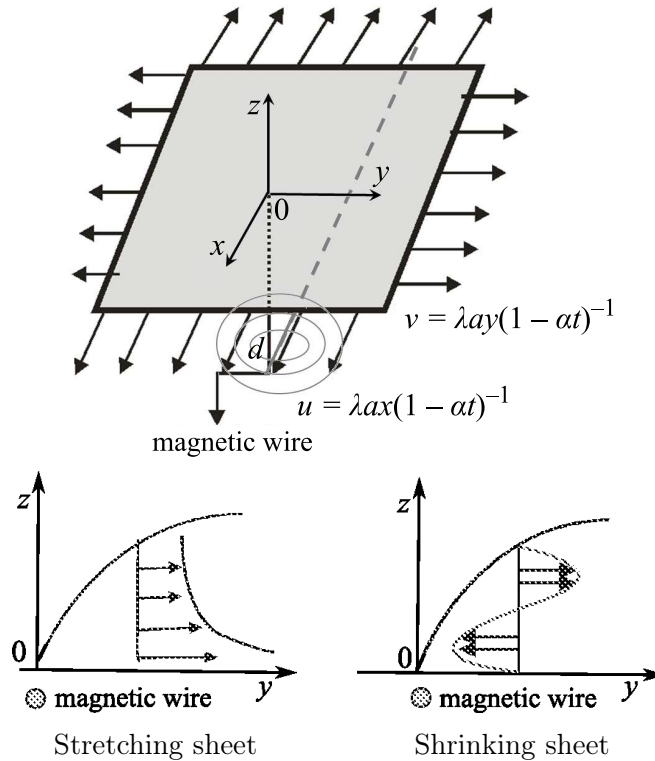


FIG. 1. Geometry of the model.

The governing equations of the unsteady three-dimensional flow of viscous incompressible biomagnetic fluid and heat transfer equations under the influence of magnetic field are [11, 13, 17, 37]:

Continuity equation:

$$(2.1) \quad \frac{\partial u}{\partial x} + \frac{\partial v}{\partial y} + \frac{\partial w}{\partial z} = 0.$$

Momentum equation:

$$(2.2) \quad \frac{\partial u}{\partial t} + u \frac{\partial u}{\partial x} + v \frac{\partial u}{\partial y} + w \frac{\partial u}{\partial z} = -\frac{1}{\rho} \frac{\partial p}{\partial x} + \nu \frac{\partial^2 u}{\partial z^2},$$

$$(2.3) \quad \frac{\partial v}{\partial t} + u \frac{\partial v}{\partial x} + v \frac{\partial v}{\partial y} + w \frac{\partial v}{\partial z} = -\frac{1}{\rho} \frac{\partial p}{\partial y} + \frac{1}{\rho} \mu_0 M \frac{\partial H}{\partial y} + \nu \frac{\partial^2 v}{\partial z^2},$$

$$(2.4) \quad \frac{\partial w}{\partial t} + u \frac{\partial w}{\partial x} + v \frac{\partial w}{\partial y} + w \frac{\partial w}{\partial z} = -\frac{1}{\rho} \frac{\partial p}{\partial z} + \frac{1}{\rho} \mu_0 M \frac{\partial H}{\partial z} + \nu \frac{\partial^2 w}{\partial z^2}.$$

Energy equation:

$$(2.5) \quad \rho C_p \left(\frac{\partial T}{\partial t} + u \frac{\partial T}{\partial x} + v \frac{\partial T}{\partial y} + w \frac{\partial T}{\partial z} \right) + \mu_0 T \frac{\partial M}{\partial T} \left(v \frac{\partial H}{\partial y} + w \frac{\partial H}{\partial z} \right) \\ = k \left(\frac{\partial^2 T}{\partial x^2} + \frac{\partial^2 T}{\partial y^2} + \frac{\partial^2 T}{\partial z^2} \right) + \mu \varphi,$$

where φ is the dissipation function and is given by the expression mentioned in TZIRTZILAKIS and KAFOUSSIAS [17]

$$(2.6) \quad \varphi = 2 \left[\left(\frac{\partial u}{\partial x} \right)^2 + \left(\frac{\partial v}{\partial y} \right)^2 + \left(\frac{\partial w}{\partial z} \right)^2 \right] + \left[\left(\frac{\partial v}{\partial z} \right)^2 + \left(\frac{\partial u}{\partial z} \right)^2 \right].$$

The initial and boundary conditions for the velocity, temperature and pressure are:

$$(2.7) \quad t < 0 : u(x, y, z) = 0, v(x, y, z) = 0, w(x, y, z) = 0 \quad \text{for any } x, y, z, \\ t \leq 0 : u = u_w(x, t) = \lambda a x (1 - \alpha t)^{-1}, v = v_w(y, t) = \lambda a y (1 - \alpha t)^{-1}, \\ w = 0, T = T_w \text{ at } z = 0,$$

$$(2.8) \quad u \rightarrow 0, v \rightarrow 0, T \rightarrow T_c, p + \frac{1}{2} \rho q^2 = p_\infty = \text{const as } z \rightarrow \infty.$$

Here $q = (u, v, w)$ are the velocity of the fluid in x, y and z axis, respectively. t is the time, a is positive constants, $p, \rho, \mu, \nu, \alpha, \lambda, \mu_0, C_p, k, M$ are the pressure, density, dynamic viscosity, kinematic viscosity, unsteadiness parameter, stretching parameter, magnetic permeability, specific heat at constant pressure, thermal conductivity and magnetization, respectively. Note that for $\lambda > 0$ the sheet is stretching whereas for $\lambda < 0$ the sheet is shrinking.

The terms $\mu_0 M \frac{\partial H}{\partial y}$ and $\mu_0 M \frac{\partial H}{\partial z}$ in (2.3) and (2.4), respectively, represent the magnetic force in y and z directions which is known as Kelvin forces and the term $\mu_0 T \frac{\partial M}{\partial T} \left(v \frac{\partial H}{\partial y} + w \frac{\partial H}{\partial z} \right)$ in (2.5) represents the Joule heating and the thermal power per unit volume.

The magnetic wire is located below the sheet at a distance d which generates the magnetic field whose components are [17]:

$$H_y(y, z) = -\frac{\gamma}{2\pi} \frac{z + d}{y^2 + (z + d)^2} \quad \text{and} \quad H_z(y, z) = \frac{\gamma}{2\pi} \frac{y}{y^2 + (z + d)^2}.$$

Therefore, the magnitude $\|H\| = H$ of the magnetic field is given by

$$(2.9) \quad H(x, y, z) = H(y, z) = [H_y^2 + H_z^2]^{1/2} = \frac{\gamma}{2\pi} \frac{1}{\sqrt{y^2 + (z + d)^2}}$$

The flow behavior of the biofluid is affected by the magnetic field which is described by the magnetization M . In this analysis, we consider that the magnetization varies with the magnetic field intensity H and temperature T and also we use the magnetization equation proposed by TZIRTZILAKIS and KAFOUSSIAS [17] and MATSUKI *et al.* [34]

$$(2.10) \quad M = KH(T_c - T).$$

3. Similarity solution for momentum and heat transfer equations

We introduce the following non-dimensional variables as HAFIDZUDDIN *et al.* [40] and TZIRTZILAKIS and KAFOUSSIAS [17]

$$(3.1) \quad \begin{cases} \xi(x) = \sqrt{\frac{a}{\nu(1-\alpha t)}} x, \\ \zeta(y) = \sqrt{\frac{a}{\nu(1-\alpha t)}} y, \\ \eta(z) = \sqrt{\frac{a}{\nu(1-\alpha t)}} z, \end{cases}$$

$$(3.2) \quad u = \frac{ax}{1-\alpha t} f'(\eta), \quad v = \frac{ay}{1-\alpha t} g'(\eta), \quad w = -\sqrt{\frac{a\nu}{1-\alpha t}} (f(\eta) + g(\eta)).$$

where primes denote derivatives with respect to η . The continuity equation (2.1) is satisfied using the similarity variables (3.2). The dimensionless pressure $P(\xi, \zeta, \eta)$ and temperature $\theta(\xi, \zeta, \eta)$ of the magnetic fluid are given by the following expressions:

$$(3.3) \quad P(\xi, \zeta, \eta) = \frac{p}{\frac{a\mu}{1-\alpha t}} = P_1(\eta) + \xi P_2(\eta) + \xi^2 P_3(\eta) + \zeta P_4(\eta) + \zeta^2 P_5(\eta),$$

$$(3.4) \quad \theta(\xi, \zeta, \eta) = \frac{T_c - T}{T_c - T_w} = \theta_1(\eta) + \xi \theta_2(\eta) + \xi^2 \theta_3(\eta) + \zeta \theta_4(\eta) + \zeta^2 \theta_5(\eta).$$

The dimensionless form of the equation (2.9) is

$$(3.5) \quad H(\zeta, \eta) = \frac{\gamma}{2\pi} \sqrt{\frac{a}{\nu(1-\alpha t)}} \left[\frac{1}{\eta + \delta} - \frac{1}{2} \frac{\zeta^2}{(\eta + \delta)^3} \right],$$

where δ is the dimensionless distance of the dipole from the ξ -axis $\delta = d\sqrt{\frac{a}{\nu(1-\alpha t)}}$ we also have

$$(3.6) \quad \frac{\partial H}{\partial \zeta} = -\frac{\gamma}{2\pi} \frac{a}{\nu(1-\alpha t)} \frac{\zeta}{(\eta + \delta)^3}$$

and

$$(3.7) \quad \frac{\partial H}{\partial \eta} = \frac{\gamma}{2\pi} \frac{a}{\nu(1-\alpha t)} \left[-\frac{1}{(\eta + \delta)^2} + \frac{3}{2} \frac{\zeta^2}{(\eta + \delta)^4} \right].$$

By substituting equation (2.10) and all the above expressions (3.1)–(3.7) into the momentum equations (2.2)–(2.4) and energy equation (2.5), and equating the coefficients of equal power of $\xi, \xi^2, \zeta, \zeta^2$, we get the following system of equations:

$$(3.8) \quad f''' + (f + g)f'' - f'^2 - 2P_3 - A(f' + \frac{\eta}{2}f'') = 0,$$

$$(3.9) \quad g''' + (f + g)g'' - g'^2 - 2P_5 - A(g' + \frac{\eta}{2}g'') - \frac{\beta\theta_1}{(\eta + \delta)^4} = 0,$$

$$(3.10) \quad P_1' + f'' + g'' + (f + g)(f' + g') + \frac{\beta\theta_1}{(\eta + \delta)^3} - \frac{A}{2}[(f + g) + \eta(f' + g')] = 0,$$

$$(3.11) \quad P_3' + \frac{\beta\theta_3}{(\eta + \delta)^3} = 0,$$

$$(3.12) \quad P_5' + \frac{\beta\theta_5}{(\eta + \delta)^3} - \frac{2\beta\theta_5}{(\eta + \delta)^5} = 0,$$

$$(3.13) \quad \theta_1'' + P_r \left[(f + g) - \frac{1}{2}A\eta \right] \theta_1' + 2(\theta_3 + \theta_5) - \frac{\delta^2\beta\lambda_a(\varepsilon - \theta_1)}{(\eta + \delta)^3}(f + g) - 4\delta^2\lambda_a(f'^2 + g'^2 + f'g') = 0,$$

$$(3.14) \quad \theta_3'' + P_r \left[(f + g) - \frac{1}{2}A\eta \right] \theta_3' - P_r(A + 2f')\theta_3 + \frac{\delta^2\beta\lambda_a}{(\eta + \delta)^3}(f + g)\theta_3 - \delta^2\lambda_a f''^2 = 0,$$

$$(3.15) \quad \theta_5'' + P_r \left[(f + g) - \frac{1}{2}A\eta \right] \theta_5' - P_r(A + 2g')\theta_5 + \delta^2\beta\lambda_a \left[\left(\frac{g'}{(\eta + \delta)^4} + 2\frac{f + g}{(\eta + \delta)^5} \right) (\varepsilon - \theta_1) + \frac{f + g}{(\eta + \delta)^3} \theta_5 \right] - \delta^2\lambda_a g''^2 = 0.$$

Also, the boundary conditions (2.7) and (2.8) become

$$(3.16) \quad f' = \lambda, \quad g' = \lambda, \quad \theta_1 = 1, \quad \theta_3 = \theta_5 = 0, \quad f = g = 0 \quad \text{at } \eta =,$$

$$(3.17) \quad f' \rightarrow 0, \quad g' \rightarrow 0, \quad P_1 \rightarrow P_\infty, \quad P_3 = P_5 = 0 \quad \text{as } \eta \rightarrow \infty$$

The dimensionless parameters are:

$$\begin{aligned} P_r &= \frac{\mu c_p}{k} && \text{Prandtl number,} \\ \lambda_a &= \frac{\mu^3}{\rho^2 k (T_c - T_w) d^2} && \text{viscous dissipation parameter,} \\ \varepsilon &= \frac{T_c}{T_c - T_w} && \text{dimensionless Curie temperature,} \\ \beta &= \frac{\gamma^2}{4\pi^2} \frac{K \mu_0 (T_c - T_w) \rho}{\mu^2} && \text{ferromagnetic interaction parameter,} \\ \delta &= d \sqrt{\frac{a}{\nu(1 - \alpha t)}} && \text{dimensionless distance,} \\ A &= \frac{\alpha}{a} && \text{dimensionless unsteadiness parameter.} \end{aligned}$$

For the present work, when ($A > 0$) we have the case of the accelerated flow whereas for ($A < 0$) we have the decelerated flow.

4. Numerical method

The essential features of the numerical technique used in the present paper are the following: (i) it is based on the common finite difference method with central differencing (ii) on a tridiagonal matrix manipulation and (iii) on an iterative procedure. This methodology was developed by KAFOUSSIAS and WILLIAMS [35]. The equations (3.8)–(3.9) are highly nonlinear. So, firstly we consider the first momentum equation and reduce it to a second order linear differential equation by considering

$$F(x) = f'(\eta), \quad F'(x) = f''(\eta), \quad F''(x) = f'''(\eta).$$

Now we rewrite Eq. (3.8) as follows

$$\begin{aligned} &\Rightarrow F''(x) + (f + g)F'(x) - f'F(x) - 2P_3 - A \left(F(x) + \frac{\eta}{2} F'(x) \right) = 0 \\ &\Rightarrow F''(x) + \left((f + g) - \frac{\eta}{2} A \right) F'(x) - (f' + A)F(x) - 2P_3 = 0, \end{aligned}$$

which is of the form

$$(4.1) \quad P(x)F''(x) + Q(x)F'(x) + R(x)F(x) = S(x),$$

where

$$P(x) = 1, \quad Q(x) = f + g - \frac{\eta}{2}A, \quad R(x) = -(f' + A), \quad S(x) = 2P_3.$$

In an analogous manner all equations of the system can be reduced in this form of equation (4.1) except for equations (3.10)–(3.12) which are already the first order differential equations. This method is presented with more details in KAFOUSSIAS and WILLIAMS [35] and used in the studies of TZIRTZILAKIS and KAFOUSSIAS [14, 17], and MURTAZA *et al.* [37].

To start the solution procedure we first have to set initial guesses for $f'(\eta)$, $g'(\eta)$, $\theta_1(\eta)$, $\theta_3(\eta)$, $\theta_5(\eta)$ between $\eta = 0$ and $\eta = \eta_\infty$ ($\eta_\infty \rightarrow \infty$) which should obviously satisfy the boundary conditions (3.16) and (3.17). For the present problem we insert the following initial guesses:

$$f'(\eta) = g'(\eta) = \left(\lambda - \frac{\eta}{\eta_\infty} \right), \quad \theta_1(\eta) = \left(1 - \frac{\eta}{\eta_\infty} \right),$$

$$\theta_3(\eta) = \theta_5 = 0.5 \left(\frac{\eta}{\eta_\infty} \right) \left(1 - \frac{\eta}{\eta_\infty} \right).$$

By integration of $f'(\eta)$ we determine the value of $f(\eta)$. Hereafter we assume that f , g , P_3 , P_5 , θ_1 are known and calculate new estimations for $f'(\eta)$, $f'_{\text{new}}(\eta)$ and $g'(\eta)$, $g'_{\text{new}}(\eta)$. These values are used for new inputs, the profiles are updated and so on. Finally, the solution is achieved iteratively until the criterion of convergence is satisfied.

After $f'(\eta)$ is obtained the solution of the energy equation (3.13) with boundary conditions (3.16) and (3.17) is solved by using the same algorithm, but without iteration now as far as Eq. (3.13) is linear. Equation (3.13) is

$$\theta_1'' + P_r \left[(f + g) - \frac{1}{2}A\eta \right] \theta_1' + 2(\theta_3 + \theta_5)$$

$$- \frac{\delta^2 \beta \lambda_a (\varepsilon - \theta_1)}{(\eta + \delta)^3} (f + g) - 4\delta^2 \lambda_a (f'^2 + g'^2 + f'g') = 0,$$

which can be written as

$$\theta_1'' + P_r \left[(f + g) - \frac{1}{2}A\eta \right] \theta_1' + \frac{\delta^2 \beta \lambda_a}{(\eta + \delta)^3} (f + g) \theta_1$$

$$= -2(\theta_3 + \theta_5) + \frac{\delta^2 \beta \lambda_a \varepsilon}{(\eta + \delta)^3} (f + g) + 4\delta^2 \lambda_a (f'^2 + g'^2 + f'g').$$

By setting $y(\eta) = \theta_1(\eta)$ is again a second-order linear differential equation of the form

$$P(x)F''(x) + Q(x)F'(x) + R(x)F(x) = S(x),$$

where

$$P(x) = 1, \quad Q(x) = P_r \left[(f + g) - \frac{1}{2}A\eta \right], \quad R(x) = \frac{\delta^2 \beta \lambda_a}{(\eta + \delta)^3} (f + g),$$

$$S(x) = -2(\theta_3 + \theta_5) + \frac{\delta^2 \beta \lambda_a \varepsilon}{(\eta + \delta)^3} (f + g) + 4\delta^2 \lambda_a (f'^2 + g'^2 + f'g').$$

Considering $f, f', g, g', \theta_3, \theta_5$ known, we obtain a new approximation $\theta_{1\text{new}}$ for θ_1 and this process continues until a convergence is attained up to a small quantity ε and finally we obtain θ_1 .

In this problem we use the discretization step $\Delta\eta = 0.01$ and by trial and error we consider the value of $\eta_\infty = 6$, and the convergence criterion $\varepsilon = 10^{-4}$ defined as

$$\varepsilon = \max_{i=1, N} \left(\left| \frac{f_{\text{old}}(i) - f_{\text{new}}(i)}{f_{\text{old}}(i)} \right| \right).$$

5. Results and discussions

In this paper, the unsteady biomagnetic fluid flow along a three dimensional stretching/shrinking sheet under the action of a magnetic field has been investigated numerically. The governing parameters such as unsteadiness parameter A , stretching parameter λ , Prandtle number P_r , and ferromagnetic interaction parameter β have a significant impact on flow and heat transfer. As far as the values of the magnetic parameters are concerned, there have been extended discussions in various studies for the possible case scenarios corresponding to plausible physical problems [13, 14, 36–39]. Especially the biomagnetic interaction parameter β can take a quite large range of values depending on the magnetic field gradient. So, for the fluid which is considered to be blood we have that:

$$\rho = 1050 \text{ kg/m}^3, \quad \mu = 3.2 \times 10^{-3} \text{ kg} \cdot \text{m}^{-1}\text{s}^{-1} \text{ [39]},$$

$$C_p = 14.65 \text{ J} \cdot \text{kg}^{-1} \cdot \text{K}^{-1}, \quad k = 2.2 \times 10^{-3} \text{ J} \cdot \text{m}^{-1}\text{s}^{-1}\text{K}^{-1} \text{ [36]},$$

and hence

$$P_r = \frac{\mu C_p}{k} = 21,$$

for a human body temperature [38] $T_w = 37^\circ\text{C}$, whereas the body Curie temperature is $T_c = 41^\circ\text{C}$, hence the dimensionless temperature is $\varepsilon = 78.5$.

The ferromagnetic number β , is defined as

$$\beta = \frac{I^2 K \mu_0 (T_c - T_w) \rho}{4\pi^2 \mu^2} = \frac{M_s B_s \rho d^2}{\mu^2},$$

where $M_s = KH(0,0)(T_c - T_w)$, $B_s = \mu_0 H(0,0)$, $H(0,0)$ are the magnetization, the magnetic field induction and the magnetic field strength intensity at the wall, respectively.

For the magnetic field 1T to 10T, the blood has reached magnetization of 40 Am^{-1} [13]. The ferromagnetic interaction parameter is calculated from the above relation and the corresponding range is from $\beta = 1 \times 10^3$ to 1×10^5 . Note that $\beta = 0.0$ corresponds to the hydrodynamic flow.

In order to verify the accuracy of the present method, the values of skin frictions ($f''(0), g''(0)$) compared with the results of HAFIZUDDIN *et al.* [40] and DEVI *et al.* [41], for $\beta = 0$ and $f'(0) = 1, g'(0) = 0.5$. The comparison indicates excellent agreement with previous data.

Table 1. The value of skin friction coefficients $f''(0), g''(0)$ varying with unsteadiness parameter.

A	DEVI <i>et al</i> [41]		HAFIZUDDIN <i>et al.</i> [40]		Present results	
	$-f''(0)$	$-g''(0)$	$-f''(0)$	$-g''(0)$	$-f''(0)$	$-g''(0)$
-1.0	0.7912	0.2956	0.7912	0.2956	0.79127	0.29566
-0.75	0.8673	0.3384	0.8673	0.3384	0.86731	0.33839
-0.5	0.9430	0.3809	0.9430	0.3809	0.94301	0.38092
0.25	1.0183	0.4232	1.0183	0.4232	1.01833	0.42325
0.0	1.0931	0.4652	1.0931	0.4652	1.09323	0.46533
0.25	1.1674	0.5059	1.1674	0.5059	1.16753	0.50706
0.5	1.2407	0.5480	1.2407	0.5480	1.24074	0.54806
0.75	1.3122	0.5878	1.3122	0.5878	1.31217	0.58784
1.0	1.3814	0.6261	1.3814	0.6261	1.38132	0.62604

Figures 2–4 show the effect of the unsteadiness parameter on velocity and temperature profiles in the reducing mode ($A < 0$) and accelerated mode ($A > 0$).

In Fig. 2, we observe the velocity profiles for the variation of the unsteadiness parameter for the stretching/shrinking sheet, respectively. For the decelerated flow ($A < 0$), the fluid velocity increases with the increment of the unsteadiness parameter A and this behavior happens approximately near the wall within the region ($\eta < 1.2$) whereas, far away from the wall this behavior is reversed. On the other hand, for the accelerated flow ($A > 0$), the velocity is decreased with the increment of the unsteadiness parameter A in the whole region.

Figure 3 shows the velocity profile $g'(\eta)$ for y axis. It is evident from the plots that for the decelerated flow ($A < 0$), the velocity decreases with the in-

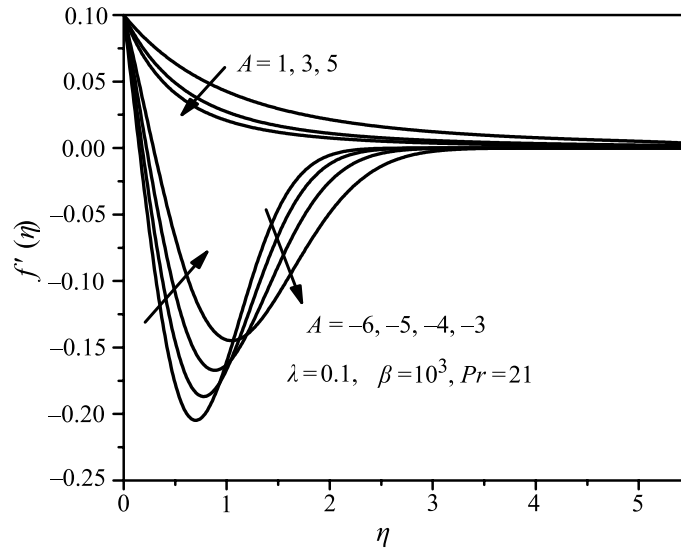


FIG. 2. The velocity profile for $f'(\eta)$ for different values of unsteadiness parameter A .

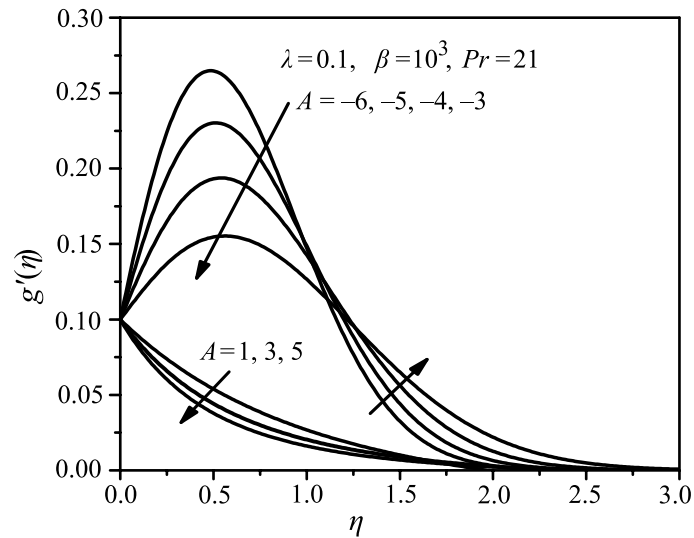


FIG. 3. The velocity profile for $g'(\eta)$ for different values of unsteadiness parameter A .

crement of the unsteadiness parameter near the wall and the opposite behavior is observed away from the boundary, for $\eta > 1.25$.

For the accelerated flow, the increment of the unsteadiness parameter results in the decrement of the boundary layer thickness in the whole region. Figure 4 presents the velocity profile $-(f(\eta) + g(\eta))$ for the z axis. We observe that for $A < 0$, the velocity is found to decrease with the increment of the unsteadiness

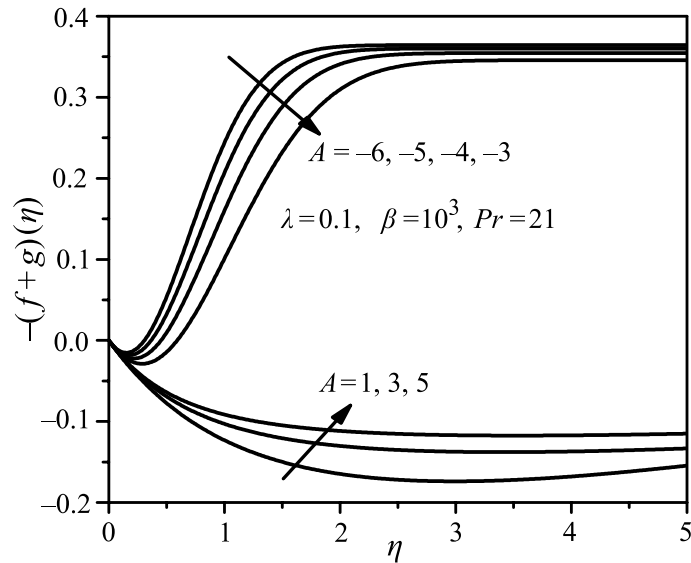


FIG. 4. The velocity profile for $-(f(\eta)+g(\eta))$ for different values of unsteadiness parameter A .

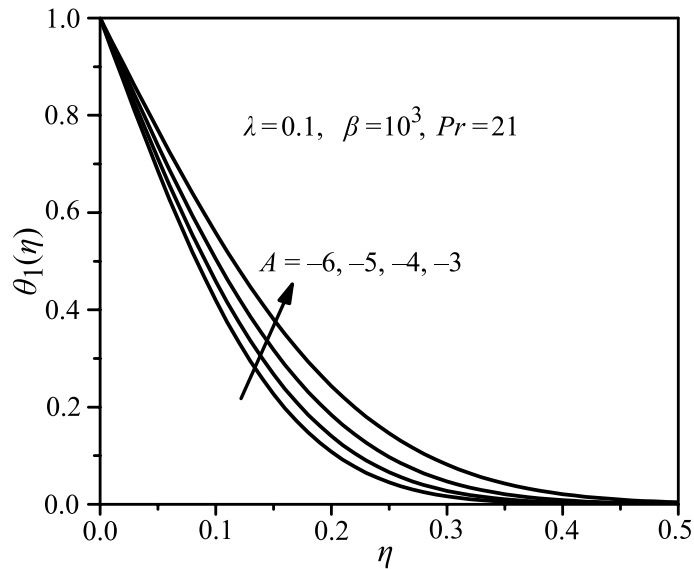


FIG. 5. The temperature profile $\theta_1(\eta)$ for different values of unsteadiness parameter A .

ness parameter. For the accelerated flow the boundary layer thickness decreases monotonically with the increment of the unsteadiness parameter A .

Figure 5 demonstrates the temperature profiles $\theta_1(\eta)$, for various values of the unsteadiness parameter for the decelerated flow. The temperature profile $\theta_1(\eta)$ is increased with the increment of the unsteadiness parameter.

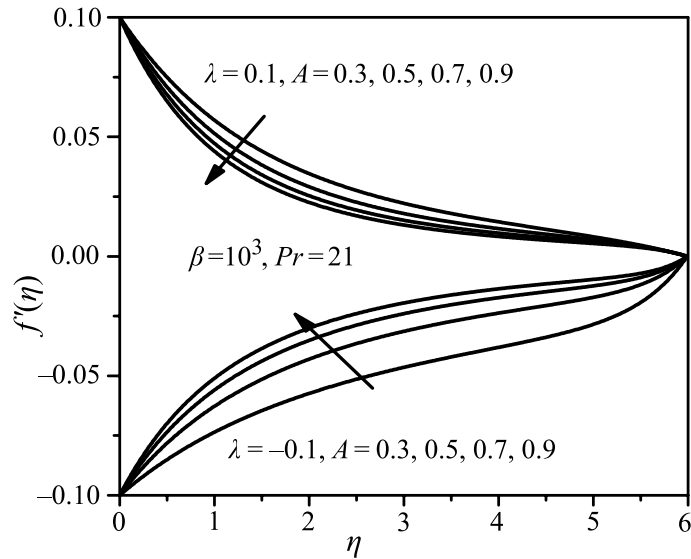


FIG. 6. The velocity profile for $f'(\eta)$ for different values of unsteadiness parameter A with stretching/shrinking sheet.

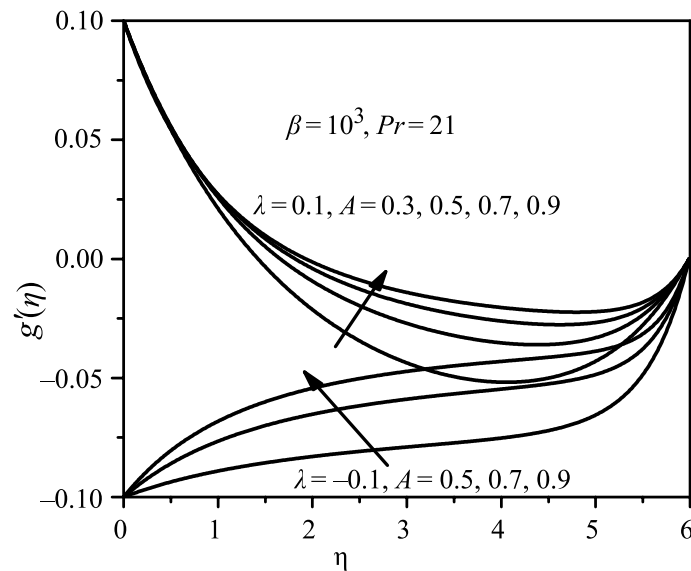


FIG. 7. The velocity profile for $g'(\eta)$ for different values of unsteadiness parameter A with stretching/shrinking sheet.

Figures 6–13 show the combine impact of the stretching and shrinking sheet for various parameters. In Fig. 6 we see that for a stretching sheet, the velocity profile decreases with the increment of the unsteadiness parameter but this result

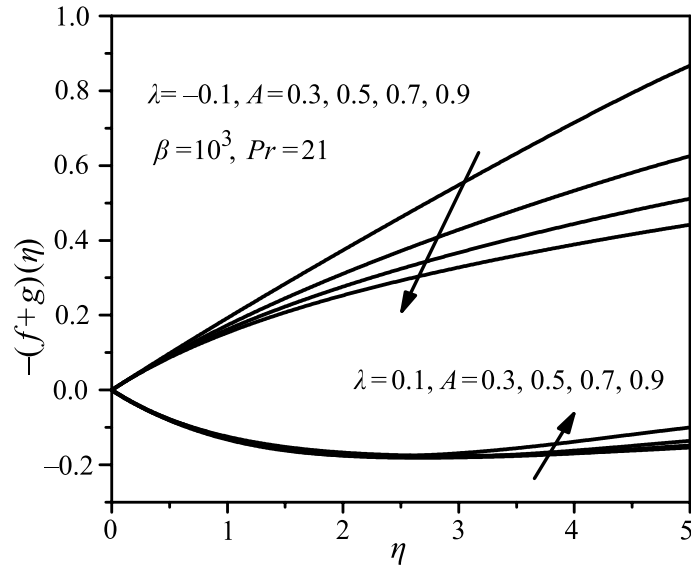


FIG. 8. The velocity profile for $-(f(\eta) + g(\eta))$ for different values of unsteadiness parameter A with stretching/shrinking sheet.

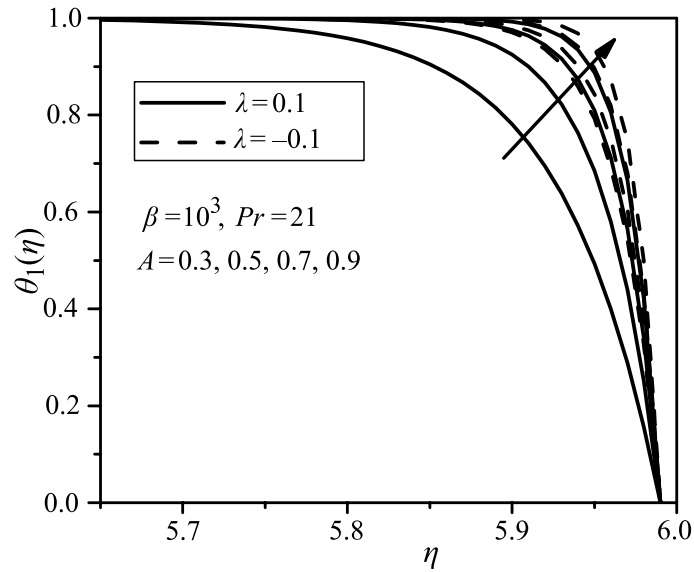


FIG. 9. The temperature profile $\theta_1(\eta)$ for different values of unsteadiness parameter A with stretching/shrinking sheet.

is reversed for the shrinking sheet. Hence, we conclude that for the stretching sheet, the increment of the unsteadiness parameter results in resistance of the flow, i.e., reduction of the momentum boundary layer thickness.

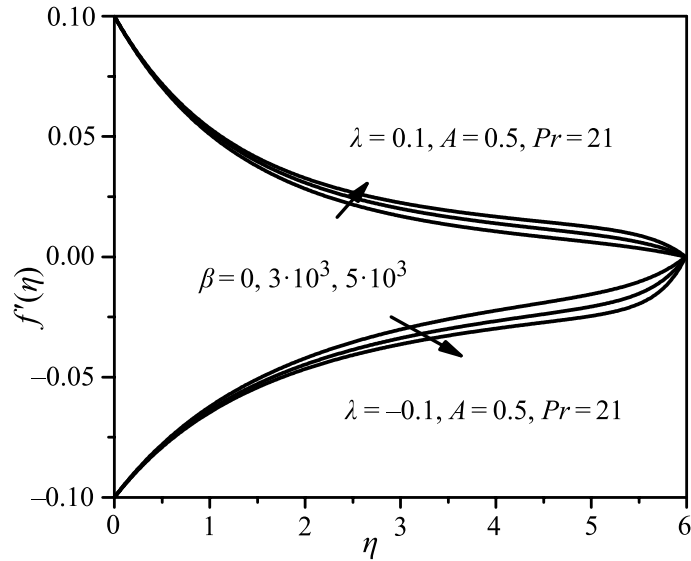


FIG. 10. The velocity profile $f'(\eta)$ of stretching/shrinking sheet with different ferromagnetic parameter β .

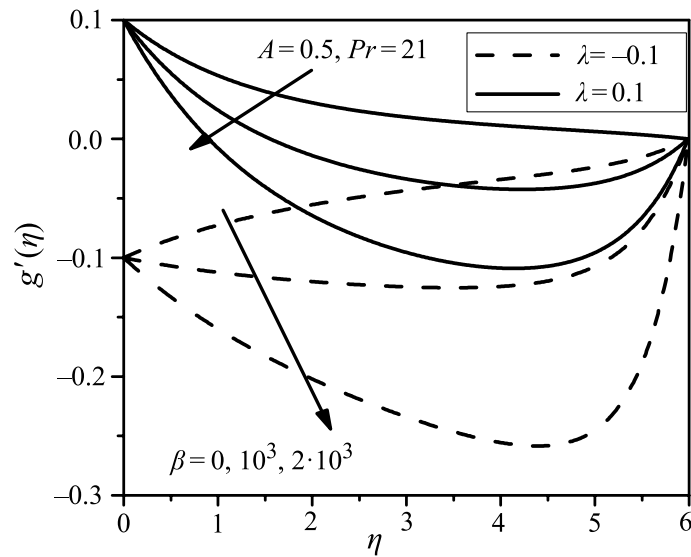


FIG. 11. The velocity profile for $g'(\eta)$ of stretching/shrinking sheet with different ferromagnetic parameter β .

From Fig. 7, we observe that increasing the unsteadiness parameter results in increment of the velocity profile $g'(\eta)$ for both stretching and shrinking cases. On the other hand, Fig. 8 shows that the increasing of the unsteadiness parameter

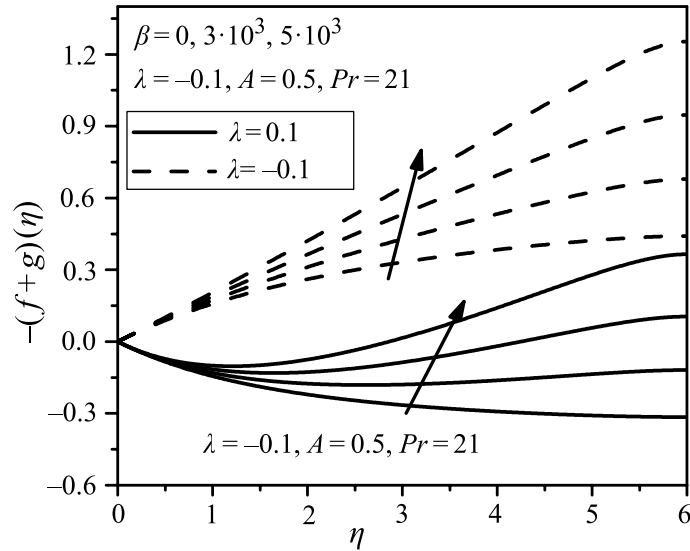


FIG. 12. The velocity profile $-(f(\eta) + g(\eta))$ for different values of ferromagnetic parameter β with stretching/shrinking sheet.

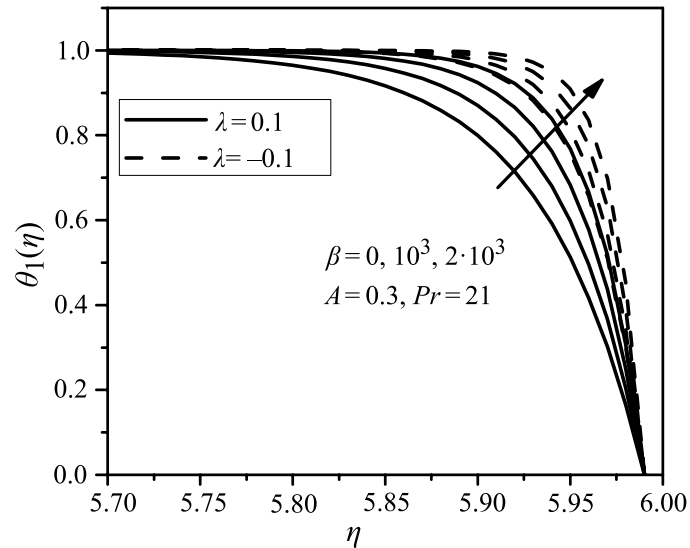
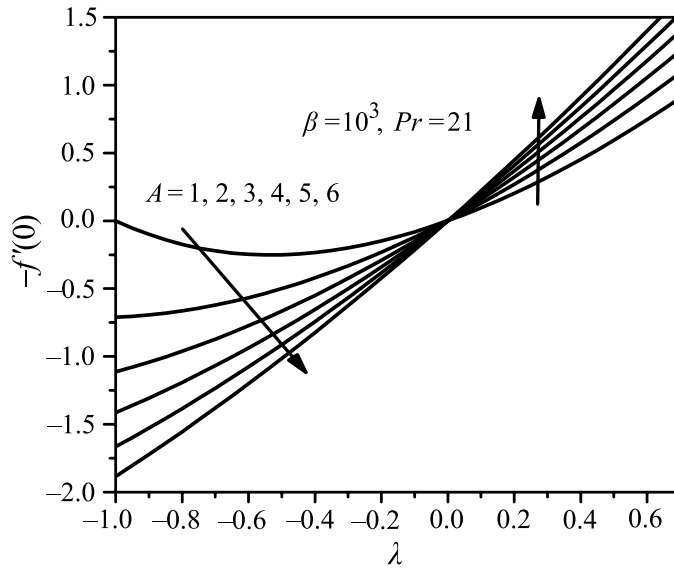
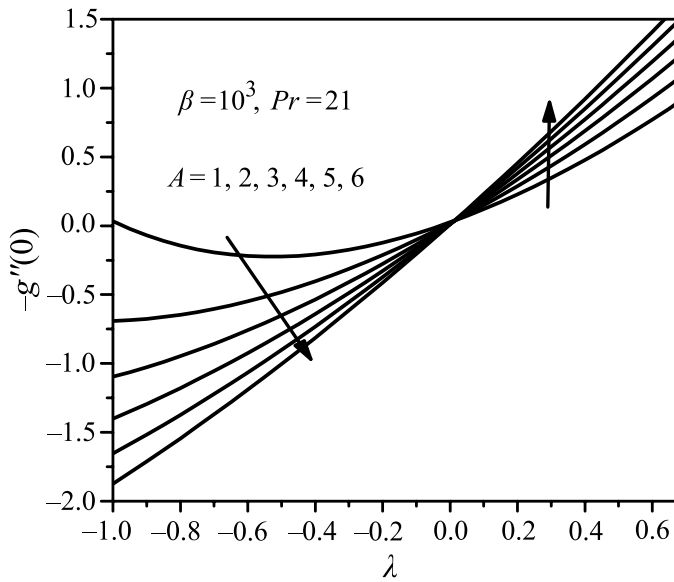


FIG. 13. The temperature profile $\theta_1(\eta)$ for different values of ferromagnetic parameter β with stretching/shrinking sheet.

results in decrement of the distribution of the velocity profile $-(f(\eta) + g(\eta))$ for the shrinking case whereas, the opposite occurs for the stretching case. The temperature profile $\theta_1(\eta)$ is pictured in Fig. 9. We observe that increment of the unsteadiness parameter results in increment of the temperature profile for

FIG. 14. Skin friction coefficient $-f''(0)$ with λ for different values of A .FIG. 15. Skin friction coefficient $-g''(0)$ with λ for different values of A .

both stretching and shrinking cases. In all cases the effect of the unsteadiness parameter is more effective in a shrinking sheet than the stretching one.

Figures 10–12 exhibit the impact of the magnetic field on velocity profiles for stretching and shrinking cases, respectively. We observe that for a stretch-

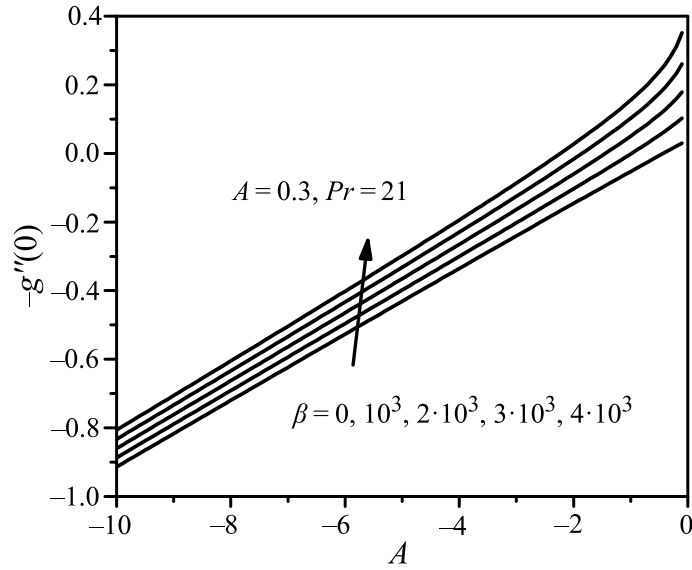


FIG. 16. Skin friction coefficient $-g''(0)$ with A for different values of β .

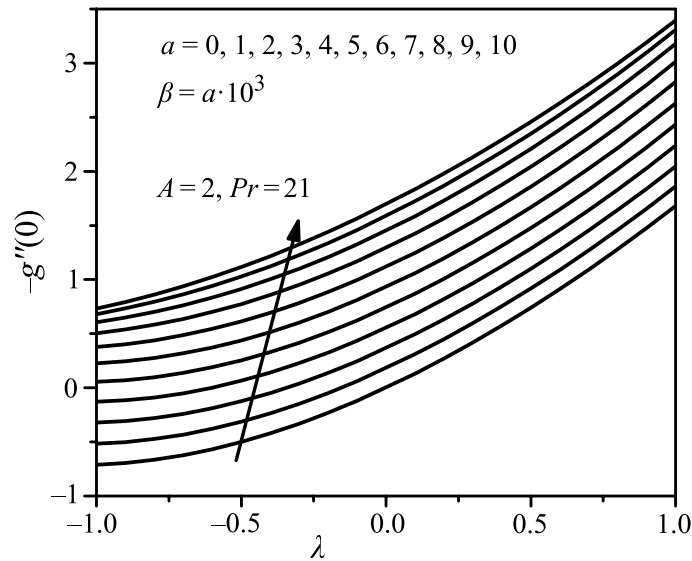


FIG. 17. Skin friction coefficient $-g''(0)$ with λ for different values of β .

ing sheet, $f'(\eta)$ and $g'(\eta)$ exhibit the reverse behavior as the magnetic field is increased. From Fig. 10 it is observed that $f'(\eta)$ is greater than that of the corresponding hydrodynamic case and it is increased with the increment of the magnetic parameter for the stretching case. The opposite is happening for the shrinking case. The behavior of $g'(\eta)$ is pictured in Fig. 11. The distribution

of $g'(\eta)$ is reduced with the increment of the magnetic parameter for shrinking and stretching sheet as well. The opposite is observed for the distributions of $-(f(\eta) + g(\eta))$ pictured in Fig. 12. This happens because the Kelvin force acts on the sheet towards the y and z axes.

Figure 13 depicts the impact of the magnetic field on temperature profiles for stretching/shrinking cases, respectively. From this figure it is apparent that the temperature profiles are increased in both stretching and shrinking cases with the increment of the magnetic field parameter. The reason of this behavior is that the increment in the magnetic field results in the reduction of the boundary layer thickness and enhances the thermal conductivity of the fluid in the stretching/shrinking sheet. This effect is more intense for the shrinking case compared to the one of the stretching case.

Figures 14 and 15 depict the skin friction coefficients ($f''(0)$, $g''(0)$) with respect to the parameter λ for various values of A . It is noted that as the unsteadiness parameter A is increased, the velocity gradients near the wall are decreased for the shrinking sheet whereas they are increased for the stretching one.

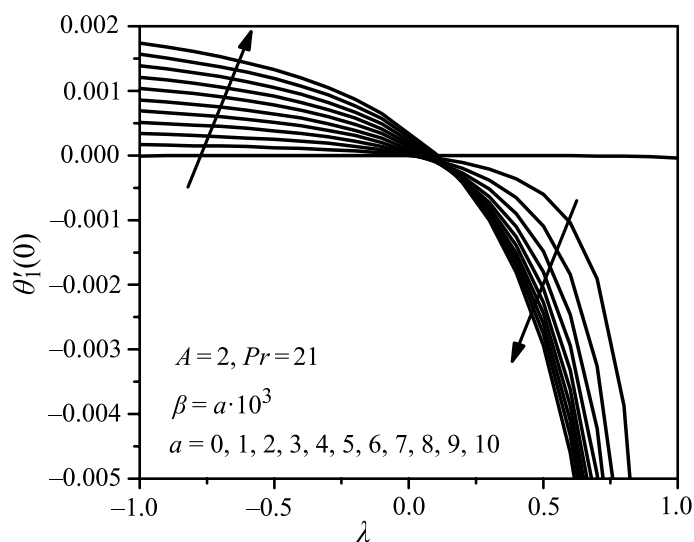


FIG. 18. Local Nusselt number $-\theta_1'(0)$ with λ for different values of ferromagnetic parameter β .

Figures 16–17 depict the skin friction coefficient ($-g''(0)$) with respect to the unsteadiness parameter A and the shrinking/stretching parameter λ for different values of the ferromagnetic parameter β . It is observed that the skin friction coefficient increases with the increment of the magnetic parameter β . Finally, Fig. 18 shows that the wall temperature gradient is increased with the increment of the ferromagnetic field parameter β in the shrinking region whereas it is reduced in the stretching region.

6. Conclusions

In this work, the three dimensional biomagnetic fluid flow past the unsteady stretching/shrinking sheet has been investigated numerically. The results indicate the following:

For accelerated flow, the velocity profile $f'(\eta)$ decreases with the increment of the unsteadiness parameter over a stretching sheet and the opposite behavior is shown for the shrinking sheet. On the other hand, the velocity profile $g'(\eta)$ is decreased for both stretching and shrinking sheets (Fig. 7) with the increment of the unsteadiness parameter.

For decelerated flow, we observed that all the flow profile has a cross flow, i.e., near the wall initially the flow motion is decreased and far away from the wall is increased and the reverse is true.

For the effect of the magnetic parameter, the velocity profile $f'(\eta)$ is increased with the increment of the magnetic number in the stretching sheet but this observation is reversed for the shrinking sheet. On the other hand, the velocity profiles $g'(\eta)$ and $-(f(\eta)+g(\eta))$ are decreased with the increment of the magnetic number in both stretching and shrinking sheets.

The thermal boundary layer thickness is increased in both stretching and shrinking sheets with the increment of the unsteady parameter and magnetic number. Note that the profile is higher in the shrinking sheet than that of the stretching one.

The skin friction coefficient is decreased/increased with the increment of the unsteady parameter for the shrinking/stretching sheet, respectively. Also skin friction is increased with the increment of the ferromagnetic number β in both sheets.

The wall temperature gradient is increased/decreased with the increase of the unsteady parameter for the shrinking/stretching sheet, respectively.

This study is intended to constitute an initial inside for all kinds of applications that deal with blood flow aiming to control the flow rate and rate of heat transfer such as magnetic drug targeting or/and magnetic hyperthermia.

Acknowledgements

The author (M. G. Murtaza) would like to thank the Ministry of Science and Technology, Bangladesh, for providing the financial support under the scheme of NST fellowship.

References

1. A.N. RUESETSKI, E.K. RUUGE, *Magnetic fluids as drug carriers: targeted transport of drugs by a magnetic field*, Journal of Magnetism and Magnetic Materials, **122**, 335–339. 1993.

2. M. LAUVA, J. PLAVINS, *Study of colloidal magnetite binding erythrocytes: prospects for cell separation*, Journal of Magnetism and Magnetic Materials, **122**, 349–353, 1993.
3. Y. HAIK, V. PAI, C.J. CHEN, *Development of magnetic device for cell separation*, Journal of Magnetism and Magnetic Materials, **194**, 254–261, 1999.
4. H.I. ANDERSSON, O.A. VANLES, *Flow of a heated ferrofluid over a stretching sheet in the presence of a magnetic dipole*, Acta Mechanica **128**, 39–47, 1998.
5. T. YASMEEN, T. HAYER, M.I. KHAN, M. IMTIAZ, A. ALSAEDI, *Ferrofluid flow by a stretched surface in the presence of magnetic dipole and homogeneous-heterogeneous reactions*, Journal of Molecular Liquids, **223**, 1000–1005, 2016.
6. A. ZEESHAN, A. MAJEED, R. ELLAHI, *Effect of magnetic dipole on viscous ferro-fluid past a stretching surface with thermal radiation*, Journal of Molecular Liquids, **215**, 549–554, 2016.
7. A. MAJEED, A. ZEESHAN, R. ELLAHI, *Unsteady ferromagnetic liquid flow and heat transfer analysis over a stretching sheet with the effect of dipole and prescribed heat flux*, Journal of Molecular Liquids, **223**, 528–533, 2016.
8. A. ZEESHAN, A. MAJEED, C. FETECAU, S. MUHAMMAD, *Effects on heat transfer of multiphase magnetic fluid due to circular magnetic field over a stretching surface with heat source/sink and thermal radiation*, Results in Physics, **7**, 3353–3360, 2017.
9. A. MAJEED, A. ZEESHAN, R. ELLAHI, *Chemical reaction and heat transfer on boundary layer Maxwell Ferro-fluid flow under magnetic dipole with Soret and suction effects*, Engineering Science and Technology, an International Journal, **20**, 1122–1128, 2017.
10. M.M. BHATTI, M. SHEIKOLESLAMI, A. ZEESHAN, *Entropy analysis on electro-kinetically modulated peristaltic propulsion of magnetized nanofluid flow through a microchannel*, Entropy, **19**, 481, 2017.
11. Y. HAIK, V. PAI, C.J. CHEN, *Biomagnetic Fluid Dynamics, in Fluid Dynamics at Interfaces*, W. Shyy and R. Narayanan [Eds.], Cambridge University Press, Cambridge, 439–452, 1999.
12. R.E. ROSENSWEIG, *Ferrohydrodynamics*, Cambridge University Press, Cambridge, 1985.
13. E.E. TZIRTZILAKIS, *A mathematical model for blood flow in magnetic field*, Physics of Fluids, **17**, (7), 077103–771018, 2005.
14. E.E. TZIRTZILAKIS, N.G. KAFOUSSIAS, *Biomagnetic fluid flow over a stretching sheet with nonlinear temperature dependent magnetization*, Journal of Applied Mathematics and Physics, **54**, 551–565, 2003.
15. I.M. ELDESOKY, *Mathematical analysis of unsteady MHD blood flow through parallel plate channel with heat source*, World Journal of Mechanics, **2**, 131–137, 2012.
16. J.C. MISRA, A. SINHA, *Effect of thermal radiation on MHD flow of blood and heat transfer in a permeable capillary in stretching motion*, Heat Mass Transfer, **49**, 617–628, 2013.
17. E.E. TZIRTZILAKIS, N.G. KAFOUSSIAS, *Three dimensional magnetic fluid boundary layer flow over a linearly stretching sheet*, Journal of Heat Transfer, **132**, 011702-1-8, 2010.
18. J. SINGH, R. RATHEE, *Analytical solution of two -dimensional model of blood flow with variable viscosity through an indented artery due to LDL effect in the presence of magnetic field*, International Journal of Physical Sciences, **5**, 12, 1857–1868, 2010.

19. K. DAS, G.C. SAHA, *Arterial MHD pulsatile flow of blood under periodic body acceleration*, Bulletin of Society of Mathematicians Banja Luka, **16**, 21–42, 2009.
20. C.S. DULAL, B. ANANDA, *Pulsatile motion of blood through an axi-symmetric artery in presence of magnetic field*, Journal of Science and Technology of Assam University, **5**, 2, 12–20, 2010.
21. M. ALI, F. AHMAD, S. HUSSAIN, *Analytical solution of unsteady mhd blood flow and heat transfer through parallel plates when lower plate stretches exponentially*, Journal of Applied Environmental and Biological Sciences, **5**, 1–8, 2015.
22. N. BACHOK, A. ISHAK, I. POP, *Unsteady boundary layer flow and heat transfer of a nonofluid over a permeable stretching/shrinking sheet*, International Journal of Heat and Mass Transfer, **55**, 2102–2109, 2012.
23. T.G. FANG, J. ZHANG, S.S. YAO, *Viscous flow over an unsteady shrinking sheet with mass transfer*, Chinese Physics Letter, **26**, 014703, 2009.
24. M.M. BHATTI, M.M. RASHIDI, *Effects of thermo-diffusion and thermal radiation on Williamson nanofluid over a porous shrinking/stretching sheet*, Journal of Molecular Liquids, **221**, 567–573, 2016.
25. M.M. BHATTI, M.M. RASHIDI, *Entropy generation with nonlinear thermal radiation in MHD boundary layer flow over a permeable shrinking/stretching sheet: numerical solution*, Journal of Nanofluids, **5**, 4, 543–548, 2016.
26. M.M. BHATTI, M.A. ABBAS, M.M. RASHIDI, *A robust numerical method for solving stagnation point flow over a permeable shrinking sheet under the influence of MHD*, Applied Mathematics and Computation, **316**, 381–389, 2018.
27. B.S. DANDAPAT, S.N. SINGH, R.P. SINGH, *Heat transfer due to permeable stretching. Wall in presence of transverse magnetic field*, Archives of Mechanics, **56**, (2), 87–101, 2004.
28. D. NIKODIJEVIC, V. NIKOLIC, Z. STAMENKOVIC, A. BORICIC, *Parametric method for unsteady two-dimensional MHD boundary-layer on a body for which temperature varies with time*, Archives of Mechanics, **63**, (1), 57–76, 2011.
29. A. MAJEED, A. ZEESHAN, T. HAYAT, *Analysis of magnetic properties of nanoparticles due to applied magnetic dipole in aqueous medium with momentum slip condition*. Neural Computing and Applications, DOI 10.1007/s00521-017-2989-5, 1–9, 2017.
30. S.R. MISHRA, P.K. PATNAIK, M.M. BHATTI, T. ABBAS, *Analysis of heat and mass transfer with MHD and chemical reaction effects on viscoelastic fluid over a stretching sheet*, Indian Journal of Physics, **91**, 1219–1227, 2017.
31. M. SHEIKOLESLAMI, M.M. BHATTI, *Forced convection of nanofluid in presence of constant magnetic field considering shape effects of nanoparticles*, International Journal of Heat and Mass Transfer, **111**, 1039–1049, 2017.
32. M. HASSAN, A. ZEESHAN, A. MAJEED, R. ELLAHI, *Particle shape effects on ferrofluids flow and heat transfer under influence of low oscillating magnetic field*, Journal of Magnetism and Magnetic Materials, **443**, 36–44, 2017.
33. Y. HAIK, V. PAI, C.J. CHEN, *Apparent viscosity of human blood in a high static magnetic field*, Journal of Magnetism and Magnetic Materials, **225**, 180, 2001.
34. H. MATSUKI, K. YAMASAWA, K. MURAKAMI, *Experimental considerations on a new automatic cooling device using temperature sensitive magnetic fluid*, IEEE Transactions on Magnetics, **13**, 1143, 1977.

-
35. N.G. KAFOUSSIAS, E.W. WILLIAMS, *An improved approximation technique to obtain numerical solution of a class of two-point boundary value similarity problems in fluid mechanics*, International Journal for Numerical Methods in Fluids, **17**, 145–162, 1999.
 36. E.E. TZIRTZILAKIS, M.A. XENOS, *Biomagnetic fluid flow in a driven cavity*, Meccanica, **48**, 187–200, 2013.
 37. M.G. MURTAZA, E.E. TZIRTZILAKIS, M. FERDOWS, *Effect of electrical conductivity and magnetization on the biomagnetic fluid flow over a stretching sheet*, Journal of Applied Mathematics and Physics, **68**, 93, 2017.
 38. V.C. LOUKOPOULOS, E.E. TZIRTZILAKIS, *Biomagnetic channel flow in spatially varying magnetic field*, International Journal of Engineering Science, **42**, 571–590, 2004.
 39. E.E. TZIRTZILAKIS, *A simple numerical methodology for BFD problems using stream function vorticity formulation*, Communications in Numerical Methods in Engineering, **24**, 683–700, 2008.
 40. H.E.M. HAFIZUDDIN, H. NAZAR, N.M. ARIFIN, I. POP, *Three-dimensional viscous flow over an unsteady permeable stretching/shrinking sheet*, Proceedings of the 3rd International Conference on Mathematical Sciences, AIP Conference Proceedings, **1602**, 422–428, 2014.
 41. S. DEVI, H.S. TAKHAR, G. NATH, *Unsteady, three-dimensional, boundary-layer flow due to a stretching surface*, International Journal of Heat and Mass Transfer, **29**, 1996–1999, 1986.

Received January 28, 2018; revised version March 12, 2018.
